ACS OMEGA

Article

http://pubs.acs.org/journal/acsodf

Fractionation and DOSY NMR as Analytical Tools: From Model Polymers to a Technical Lignin

James R. D. Montgomery, Christopher S. Lancefield, Daniel M. Miles-Barrett, Katrin Ackermann, Bela E. Bode, Nicholas J. Westwood,* and Tomas Lebl*

School of Chemistry and Biomedical Sciences Research Complex, University of St Andrews and EaStChem, North Haugh, St Andrews, Fife KY16 9ST, U.K.

Supporting Information

ABSTRACT: One key challenge hindering the valorization of lignin is its structural complexity. Artificial lignin-like materials provide a stepping stone between the simplicity of model compounds and the complexity of lignin. Here, we report an optimized synthesis of an all-G β-O-4 polymer **1** designed to model softwood lignin. After acetylation, the polymer **Ac-1(V)** was fractionated using a protocol that involved only volatile organic solvents, which left no insoluble residue. Using diffusion ordered spectroscopy NMR in combination with gel permeation chromatography, it was revealed that this fractionated material behaved like a flexible linear polymer in solution (average $\alpha > 0.5$). Acetylated kraft lignin was subsequently processed using the same fractionation protocol. By comparison with the model polymer, we propose that the acetylated kraft lignin is composed of two classes of materials that exhibit contrasting physical properties. One is comparable to the acetylated all-G β-O-4 polymer **Ac-1**, and the second has a significantly different macromolecular structure.

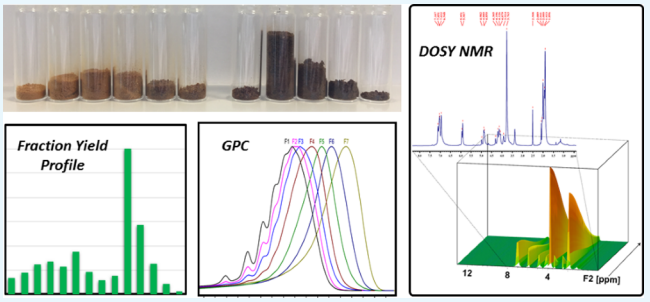

INTRODUCTION

The biorefinery concept requires that value is derived from all of the components that make up biomass as this should ensure economic viability.[1] For lignocellulosic biomass, this means that lignin, as well as the cellulose and hemicellulose fractions, must be made full use of. Numerous groups worldwide study the use of lignin either as a starting point for novel material development or as a source of renewable low-molecular-weight chemical feedstocks or new platform chemicals.[2−7] One key challenge is the complexity of lignin and the impact it has on both its chemical reactivity and analysis. For example, depolymerization of lignin by targeting the β-O-4 linkages requires two contiguous linkages of this type for monomer unit production (excluding end groups). This limits the maximum yield of monomers derived exclusively from a β-O-4 unit to around 14−36 wt % depending on the source of lignin.[8,9] To realize the full potential of lignin, we must continue to improve our understanding of its structure.

The biggest obstacle for lignin characterization is likely its heterogeneity and polydisperse nature.[10] Although heteronuclear single quantum coherence (HSQC) NMR studies of lignin have proved to be very useful for identifying various structural features and functional groups, using this method in a quantitative manner is questionable.[11] A crude lignin sample can be composed of molecules with a large span of molecular weights (MWs) that will impact on the T_1 and T_2 relaxation times of the NMR resonances. Although the effect of T_1 relaxation can be mitigated by using relaxation agents and long interscan delays, the effect of T_2 relaxation on the insensitive nuclei enhancement by polarization transfer (INEPT), that is utilized by HSQC correlations, is unavoidable.[12]

One way to simplify this inherent challenge is to "purify" the lignin in such a way that a series of fractions are formed that cover different molecular weight windows. This is referred to as *fractionation*, and a wide range of different methodologies have been developed.[13−19] The standard protocol for determining the MW of fractions is currently gel permeation chromatography (GPC), but there are fundamental limitations to this method.[20,21] For instance, structural features cannot be differentiated from each other using this analysis. In addition, calibration is typically done using polystyrene standards that do not effectively mimic the structure of lignin.[20]

Here, inspired by previous publications, we report our studies on the use of the ^{1}H-pulsed field gradient (PFG) NMR technique [diffusion-ordered spectroscopy (DOSY)] that could provide significant advantages when analyzing lignin fractions.[22−24] Our initial studies use a polymeric lignin model (an all-G β-O-4 polymer **1**, Scheme 1B) that we have prepared. After acetylation, model polymer **1** was fractionated using a new organic solvent-based approach and each fraction was analyzed using GPC, ^{1}H NMR end-group analysis, and DOSY

Received: September 1, 2017
Accepted: November 8, 2017
Published: November 30, 2017

DOI: 10.1021/acsomega.7b01287
ACS Omega 2017, 2, 8466−8474

Scheme 1. (A) 1:1 S:G β-O-4 Polymer 2 and Its Depolymerization products[8] and (B) synthesis of All-G β-O-4 Model Polymers 1(I–VIII)[a]

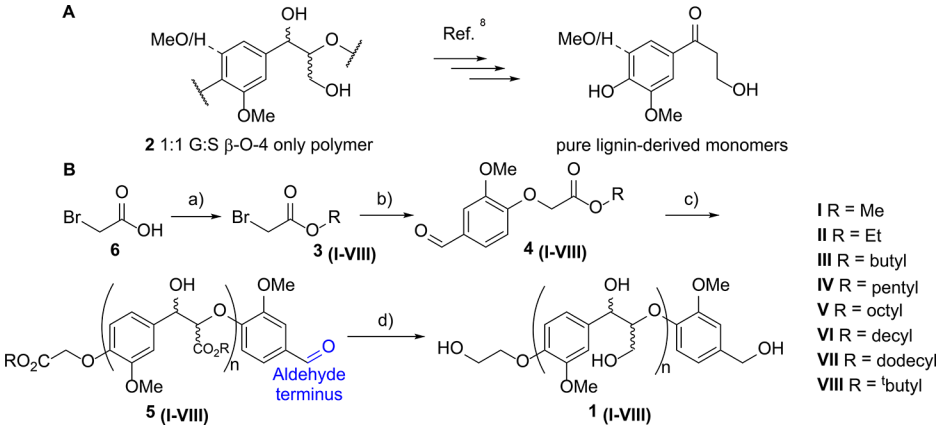

[a]Roman numerals correspond to the entries in Table 1. Methyl, ethyl, and *t*-butyl derivatives of **3** were commercially available. Reaction conditions: (a) *p*-toluene sulfonic acid (0.01 equiv), alcohol ROH (1 equiv), cyclohexane, reflux, Dean–Stark apparatus, >99% yield; (b) K_2CO_3, acetone, vanillin, reflux, 20 min, >99% yield; (c) (i) LDA, THF, −78 °C, 2 h and (ii) sat. NH_4Cl, EtOAc; and (d) (i) $NaBH_4$ (3 equiv), MeOH (9 equiv), EtOH, reflux, 50 °C, 1 h and (ii) H_2O, 6 M HCl. Alternative representation of **5** is given to highlight the end groups used to assess the degree of polymerization (DP).

Table 1. Study of Polymer Synthesis Using Different Monomer Units[a]

				GPC MW of **1** [g mol^{-1}]		
entry	R	DP **5**(I–VIII)	Isolated yield of **1**(I–VIII) (%)[b]	M_n	M_w	$Đ_M$ (M_w/M_n)
I	methyl	4.5	10	1000	1700	1.8
II	ethyl	4.9	10	1300	2700	2.1
III	butyl	4.7	16	1200	2800	2.3
IV	pentyl	5.1	26	1400	3600	2.6
V	octyl	6.2	33	2100	8000	3.8
VI	decyl	4.7	24	2200	8700	3.9
VII	dodecyl	5.1	14	1800	4400	2.5
VIII	^{t}Bu	2.2	4	1000	1400	1.4

[a]DP assessed by quantitative ^{1}H NMR. The yield corresponds to the isolated mass of **1** after purification by precipitation into diethyl ether. Number average (M_n) and weight average (M_w) MWs were assessed by GPC (g mol^{-1}). Molar mass dispersity ($Đ_M$) values were calculated by taking the ratio of the average MWs measured by GPC (M_w/M_n). [b]Corresponds to the mass of **1** isolated after being precipitated from an acetone/methanol (9:1) solution into 10 volumes of diethyl ether compared to the theoretical maximum amount.

NMR methods. The results obtained using the three techniques correlated well and encouraged us to repeat the process using a commercial kraft lignin. The analysis shows that acetylated kraft lignin can be viewed as being made up of two different sets of fractions: one set that shows properties similar to those of our acetylated all-G β-O-4 model polymer **1** and a second set that is clearly very different from this model polymer. These findings are supported by electron paramagnetic resonance (EPR) analysis of the crude kraft lignin and its acetylated fractions. Furthermore, effects of MW of lignin fractions on NMR relaxation times and intensity of resonances in HSQC correlation experiments will be discussed.

RESULTS AND DISCUSSION

The synthesis of model lignin polymers is an advanced area with methods ranging from the preparation of dehydrogenase polymers using biomimetic approaches[25] to the controlled preparation using chemical methods of less[8,26,27] or more[28] advanced lignin polymers. We have reported a robust route to a 1:1 S:G β-O-4 polymer **2** which was used to aid the development of a novel lignin depolymerization protocol (Scheme 1A).[8,28] Our polymer **2** modelled a hardwood lignin, and few synthetic challenges were encountered during its synthesis. However, given the commercial availability of softwoods and their frequent use in industrial pulping and biorefining, it was decided to prepare an all-G β-O-4 model polymer **1** for use in this study (Scheme 1B). Use of a synthesis protocol analogous to that developed for **2** yielded limited amounts of **1**, so we started by optimizing the model polymer synthesis. A more detailed experimental section can be found in the Supporting Information.

Optimization of the Synthesis of All-G β-O-4 Polymer 1. In brief, the approach used to prepare **1** started with the commercially available bromo-ester **3(II)** (R = Et, Scheme 1B). Alkylation of the phenolic oxygen in vanillin with **3(II)** gave monomer **4(II)** in nearly quantitative yield. Subsequent reaction of **4(II)** with LDA led to the formation of the polyether **5(II)**, which was carried through crude, and the aldehyde and carboxylic ester groups were reduced using sodium borohydride. Workup involved the precipitation of polymer **1(II)** from water using a 6 M hydrochloric acid solution. A low yield of **1(II)** was obtained using these conditions (10%, half of that previously reported for the synthesis of **2**[8,28]). One possible explanation for this difference was that during the polymerization reaction, **5(II)** was poorly soluble in the organic reaction solvent [tetrahydrofuran

DOI: 10.1021/acsomega.7b01287
ACS Omega 2017, 2, 8466–8474

(THF)], leading to the precipitation of low-molecular-weight chains early in the reaction. The lower MW polyether chains in **5(II)**, when reduced to give polymer **1(II)**, would also be expected to be soluble in the acidic aqueous workup solution and hence did not precipitate. It seems likely that these two factors combine to reduce the yield. As large quantities of polymer **1** were needed, optimization was required.

The only position that can be varied is the structure of the ester group in **4** (Scheme 1B). A range of bromo-esters **3(I–VIII)** was used to prepare different polymerization monomers **4(I)** and **4(III)–4(VIII)**. The methyl and ^{t}Bu derivatives of **3** were commercially available whilst the higher alkane-containing bromoesters were synthesized from bromoacetic acid **6** and the respective alkyl alcohol using Dean–Stark apparatus (quantitative yields). For consistency, all polymerizations of **4(I–VIII)** were performed on a 2 g scale in 40 mL of THF with 2 h of stirring after the addition of the freshly prepared LDA. In general, it was observed that polymer **5** precipitated less rapidly with increasing chain length of the alkyl R group in **4**. Consistent with this, the average length of the polymer chain in **5** (referred to as the DP) increased as R increased in size up to the point when R = octyl (Table 1 and Figure S1). The decyl (**4(VI)**) and dodecyl (**4(VII)**) derivatives gave polymers **5(VI)** and **5(VII)**, respectively, with smaller DPs compared to that of the octyl derivative **5(V)**. Precipitation of the polymer with a methyl side chain **5(I)** occurred very quickly, consistent with its low DP (Table 1). Branched poly(ester) **5(VIII)** gave the worst DP (2.2 units), so other branched esters were not studied. Reduction of polymers **5(I–VIII)** gave isolated yields of the final polymer **1** ranging from 4 to 33% (Table 1). A correlation between the DP of **5** and the isolated yield of **1** was observed, with model polymer **1(V)** derived from polymer **5(V)** (DP = 6.2) being obtained in the highest yield (33%) and model polymer **1(VIII)** derived from polymer **5(VIII)** (DP = 2.2) being formed in the lowest yield (4%).

The MWs (M_n and M_w) of polymer models **1(I–VIII)** were assessed by GPC. The weight average MW (M_w) of **1** varied from 1700 to 8700 g mol^{-1} whilst the number average MW (M_n) of **1** varied from 1000 to 2200 g mol^{-1}. M_n and M_w were at their highest for polymer models **1(V)** and **1(VI)**. The polymer model **1(VIII)** derived from the polymer with the branched *t*-Bu side chain **5(VIII)** gave the lowest average MWs in the series (Table 1, entry **VIII**). The polydispersity of the isolated polymer models **1** increased from 1.8 for **1(I)** to 3.9 for **1(VI)**. Values for the polydispersity of lignin are between 1.4 and 8.5[29] depending on the species of wood, suggesting that any of the polymer models prepared here could be used to mimic typical lignin MW distributions. Given the yield of production of the polymer model **1(V)** from the polymer with an octyl side chain **5(V)** (33%) and the relatively high MW and polydispersity of **1(V)**, it was decided to scale-up its synthesis, leading to the preparation of a total of 34.5 g in three batches of **1(V)**. GPC analysis showed that a reduction in the MW and polydispersity of the resulting polymer **1(V)** occurred compared to the small-scale reaction (Table S1; for HSQC assignment, see Figure S2).

Fractionation and Analysis of Softwood All-G *β*-O-4 Polymer Model 1(V). *Fractionation of Acetylated Model Polymer **Ac-1(V)**.* Having prepared a sufficient amount of polymer **1(V)**, the next stage was to identify a fractionation method. Whilst a range of protocols for lignin fractionation have been reported,[13−19] we developed an alternative approach that relied on the use of a varying ratio of two volatile organic solvents. This choice was made to enable a controllable increase in the polarity ("dissolving ability") of the solvent mixture and for the practical reason that it would decrease the amount of time required to recover the lignin fractions through the removal of the volatile solvents in each step of the process (approximately 10 min per sample was required). A previously reported protocol involved using acetone and hexane as the solvent and the antisolvent, respectively.[30] However, this fractionation selectively precipitated lignin fractions using different ratios of the solvents and was reported to leave a considerable amount of lignin unfractionated. Here, we report the selective dissolution of lignin-like polymers using a similar solvent/antisolvent system. Unfortunately, our model polymer **1(V)** was only partially soluble in the types of solvents we wanted to use, and the solubility was expected to be worse when real lignin samples were used. Because acetylation of lignin has been reported to enhance its solubility,[31] we decided to acetylate polymer **1(V)** using pyridine and acetic anhydride to give the acetylated polymer **Ac-1(V)**. Subsequent fractionation of **Ac-1(V)** was then performed by stirring the acetylated polymer in 10 volumes (v/v) of an acetone–diethyl ether solvent system. The initial concentration of acetone was 5% (v/v), and at each step of the fractionation, this was incremented by 5% until all of the polymer had dissolved (Figure S3). This also highlights a further advantage of fractionating acetylated polymers/lignin because all of the material was dissolved, leaving no insoluble residue. To the best of our knowledge, other reported fractionation procedures do not achieve this using only volatile organic solvents in a solvent/antisolvent system. Two fractionations were initially carried out on polymer **Ac-1(V)** to assess reproducibility (G-1 and G-2, Figure 1 and Table S1). Fraction yield analysis was then performed to determine the mass distribution across the fractions. In total, seven fractions were obtained for both G-1 and G-2 fractionations, with a near Gaussian distribution being observed for the isolated yields (blue and red series, Figure 1; and Table S2). The total yield of the fractionation process was 88% for G-1 and 95% for G-2 (theoretical yield, assuming 98% of material recovered at each step is 87% 0.98[7]). The slight difference in fraction yield profiles between runs may result from the contrasting overall yields (Table S2).

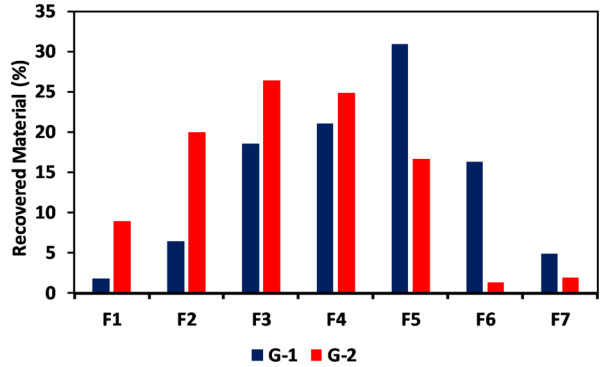

Figure 1. Mass balance of the fractions of **Ac-1(V)** performed in triplicate. The bars correspond to the first (G-1, blue) and second (G-2, red) fractionation runs. Yields are shown as percentages of the total recovered material.

***Ac-1(V)* Fraction GPC Analysis.** Average MWs (M_w and M_n) of the **Ac-1(V)** fractions were obtained by GPC using polystyrene standards sourced from Polymer Standards Service

DOI: 10.1021/acsomega.7b01287
ACS Omega 2017, 2, 8466–8474

(PSS) to generate a calibration curve.[20,32] The overlay of the chromatograms of the fractions from fractionation G-1 showed that the initial bulk material had been fractionated into seven bands of different average MWs (Figure 2). This was consistent

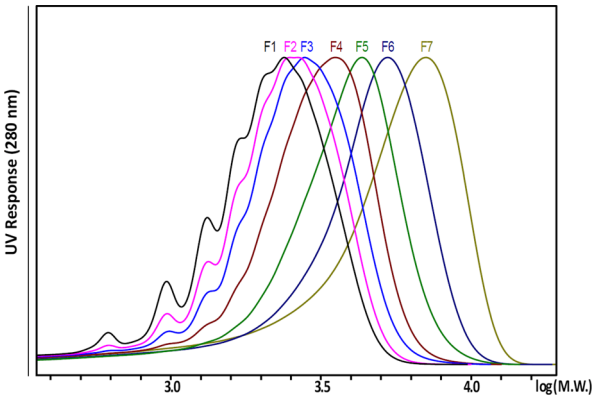

Figure 2. Overlay of GPC chromatograms of fractions derived from the first fractionation G-1 series. The analysis of these fractions was carried out in triplicate (G-1(1), Table S3). Arbitrary scaling was used in the vertical dimension to match the heights of all peaks. Overlay of chromatograms with scaling derived from isolated yields of particular fractions is shown in Figure S4.

across both fractionations (G1 and G2). To assess experimental error, this GPC analysis was performed in triplicate. The statistical analysis revealed that the maximum observed standard deviation (σ) for each fraction was within 1.6% of the mean value (Table S3, fraction F7). With the reproducibility of the analysis confirmed, subsequent analyses were not performed in triplicate.

The corresponding G-1 M_w average values (Table S4) steadily increased from 2400 g mol^{-1} (G-1 F1) to 5900 g mol^{-1} (G-1 F7). The M_n values were found to be lower ranging from 1800 g mol^{-1} (G-1 F1) to 3700 g mol^{-1} (G-1 F7). The G-2 fractionation showed a similar trend [from 1800 to 5000 g mol^{-1} (M_w) and from 1400 to 3000 g mol^{-1} (M_n) (Table S4)].

The polydispersity ($Đ_M$) across all fractionations was also calculated and gave a low value of 1.3 for early fractions (F1−F4, Table S4). From fraction F5 onward, however, $Đ_M$ of each fraction increased (see Table S4 and the Supporting Information for a more detailed discussion). Because of the uncertainties in the GPC M_n determination and the simplicity of the 1D ^{1}H NMR spectrum of **Ac-1(V)**, quantitative NMR end-group analysis was used to obtain an alternative value of M_n for comparison.

Quantitative ^{1}H NMR Analysis of Fractions of ***Ac-1(V)***. For polymers with relatively low MWs, end-group analysis by ^{1}H NMR offers a reliable alternative for measuring M_n.[33] Because all fractions derived from model polymer **Ac-1(V)** have end groups detectable by ^{1}H NMR, this method was used to compare M_n values with those obtained by GPC. Quantitative ^{1}H NMR spectra of all of the fractions derived from polymer **Ac-1(V)** were acquired. The average chain length (and the respective M_n) for each fraction was then calculated (see Figure S5 and Table S5 for details). The end-group analysis of the G-1 fractionation series showed that the M_n values increased from 1700 (F1) to 4300 (F7) g mol^{-1} (Table S6), with a significant difference between the two techniques being observed for the heavier fractions (Table S6). By substituting the M_n(NMR) value in place of the M_n(GPC) value, more consistent polydispersity values were calculated (Table S7, $Đ_M$ = 1.3 ± 0.1 for all fractions F1−F7). An analogous picture was seen for the G-2 fractionation (Table S8). Although this use of M_w and M_n values from different techniques is not suitable to accurately assess $Đ_M$, we believe that this comparison highlights a possible source of error coming from GPC. Despite these small discrepancies in M_n values, quantitative ^{1}H NMR analysis has provided additional evidence for a successful fractionation.

Diffusion ^{1}H-PFG NMR Analysis of Fractions of ***Ac-1(V)***. PFG NMR spectroscopy can be used to measure the translational diffusion of molecules. The diffusion coefficient (D) can be linked with resonances in the NMR spectrum and the corresponding structural features in the analyzed molecules. For polymers, the Mark−Houwink equation (eq 1) based on the Flory scaling relationship can be used to establish the relationship between D and MW.[34,35]

$$D = K\mathrm{MW}^{\alpha} \tag{1}$$

In eq 1, K and α are the so-called scaling parameters that depend on the macromolecular polymer structure as well as the experimental conditions, namely, solvent viscosity and temperature. The scaling parameters K and α can be obtained by analyzing a series of monodisperse polymer standards under a given set of experimental conditions and fitting the logarithmic form of the Mark−Houwink equation (eq 2) into the experimental data.

$$\log D = \alpha \log \mathrm{MW} + \log K \tag{2}$$

It should be noted that high viscosity and molecular crowding can also hinder the diffusion. Therefore, sample concentration and temperature must be controlled across a series of diffusion measurements. If concentration control is not feasible, a correction factor derived from the concentration dependence can be used.[36−38]

To the best of our knowledge, only a few examples of the application of the Mark−Houwink equation to lignin can be found in the literature.[22,23] Garver et al.[23] have studied the scaling of diffusion coefficients with the MW for unacetylated lignin fractions in 1 M NaOH and acetylated lignin in $CDCl_3$. The fractions for this study were obtained by preparative size exclusion chromatography (SEC) with 0.1 M NaOH as the mobile phase. The values of molecular scaling exponent α, 0.39 and 0.30, are found to be consistent with a very compact and branched structure of the particular lignin under study.[23]

Kraft lignin fractions obtained by preparative SEC and characterized by matrix-assisted laser desorption ionization time-of-flight mass spectrometry have been used to establish a Mark−Houwink calibration curve.[22] We decided to explore whether the fractions of model polymer **Ac-1(V)** could conform to the same relationship and whether our solvent fractionation method could be used to determine the calibration curve that is essential for the application of DOSY NMR to lignin analysis.

The average values of the diffusion coefficient D obtained for each of the fractions derived from **Ac-1(V)** in fractionation G-1 showed a strong linear correlation with both the M_w (blue line, Figure 3) and M_n (orange line) values resulted from the GPC analysis, with correlation coefficients R^2 = 0.994 and 0.993, respectively (Figure 3 and Table S10). Both calibration curves also yielded similar scaling parameters (α = 0.69 and 0.89 and log K = −7.90 and −7.32). The difference in the scaling factor α that was calculated using either the M_n(GPC) or the M_w(GPC) values was expected as $Đ_M$ of the fractions was

DOI: 10.1021/acsomega.7b01287
ACS Omega 2017, 2, 8466−8474

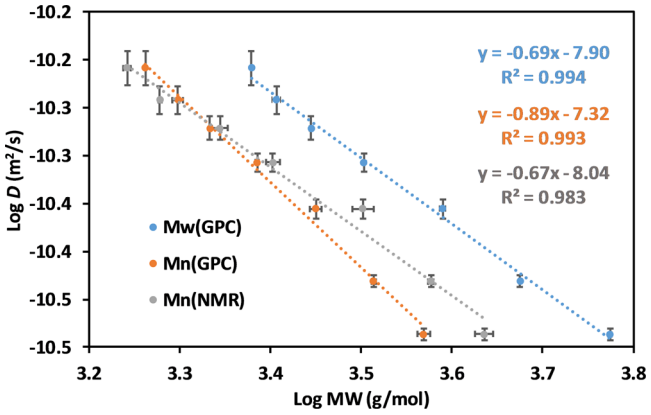

Figure 3. Comparison of M_w and M_n DOSY calibration curves for model polymer **Ac-1(V)** fractions (G-1). MW data were taken from the M_w and M_n values as measured by GPC (blue and orange lines, respectively) and the M_n values calculated from ^{1}H NMR end-group analysis (gray line). Error bars in the diffusion dimension correspond to the associated standard error of the average diffusion coefficient of each fraction. Error bars in the MW dimension correspond to the standard error of the average MW values generated by doing the analysis in triplicate.

higher than 1. The M_n data from the ^{1}H NMR end-group analysis (gray line) was also evaluated. The resulting scaling factors (α = 0.67 and log K = −8.04) were found to be comparable with those obtained using average MWs measured by GPC. To assess the error associated with fitting this data to the Mark−Houwink equation, the analysis was repeated for the G-2 fractionation data (Table S10 and Figure S7). Scaling factors α and log K for the two fractionations (G-1 and G-2) are summarized in Table 2 for comparison. For low-molecular-mass unbranched polymers such as **Ac-1(V)**, we assume that M_n derived from end-group analysis is the most reliable which is confirmed by the good reproducibility of the Mark−Houwink parameters (α = 0.66 ± 0.01 and log K = −8.04). We propose that these values could be used as empirical Mark−Houwink parameters for a quick DOSY NMR assessment of MW of light fractions of unbranched lignin with a low MW of up to about 4.5 kDa. Very similar scaling parameters with reasonable reproducibility (α = 0.70 ± 0.02 and log K = −7.82 ± 0.08) were obtained using the M_w(GPC) values. The least reliable seem to be the M_n values determined by GPC as they showed inferior reproducibility.

Kraft Lignin Fractionation and Analysis. *Kraft Lignin Fractionation.* As the simplest possible lignin-like material, **Ac-1(V)** has the potential to serve as a reference point in the tool kit for lignin characterization. We assume that the fractionation and analytical methods that are presented here could be applied to technical lignin samples. Kraft lignin was chosen for this study because (i) it represents a significant percentage of the lignin produced industrially at present and (ii) it is generally accepted to be heavily condensed and as such provides the greatest contrast to the linear **Ac-1(V)**. To investigate the reproducibility of the process, two fractionation experiments were performed (KL-1 and KL-2). To fractionate all of the kraft lignin, the concentration range of acetone in diethyl ether had to be increased from 5% up to 70%, so 14 fractions in total were obtained per fractionation. The fraction yield profiles were more complex than those obtained with **Ac-1(V)**, showing two obvious regions that must correspond to the components of kraft lignin with different physical properties (e.g., solubility, Figure 4) which seems to be in accordance with the recently

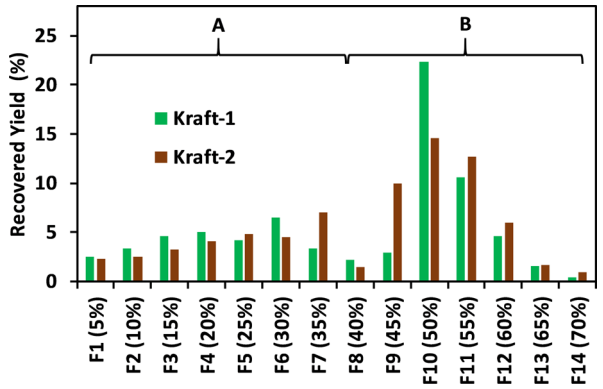

Figure 4. Fraction yield profiles of KL-1 (green series, overall yield of 89%) and KL-2 (brown series, overall yield of 85%). Two possible regions were identified: (A) fractions 1−8—approximately Gaussian distribution that, in the subsequent analysis, resulted in scaling factors similar to those of **Ac-1(V)** and (B) fractions 9−14—approximately Gaussian distribution that, in the subsequent analysis, gave scaling factors different from those of **Ac-1(V)**. The similar pattern of fraction yield profiles was taken to confirm reproducibility.

published results by Crestini et al.[10] The total yield of the lighter fractions was low (25−30%) but followed a near Gaussian distribution that was analogous to that observed for **Ac-1(V)**. Significantly higher yields of the heavier fractions were isolated, with a maximum average yield of about 25% being obtained for fraction F10. The threshold between the two

Table 2. Scaling Factors α and log K for the Two Fractionations (G-1 and G-2) of Polymer Ac-1(V) and from the Combined Correlation of the Kraft Lignin Fractionations KL-1 and KL-2[a]

	α			log K			R^2		
	M_w(GPC)	M_n(GPC)	M_n(NMR)	M_w(GPC)	M_n(GPC)	M_n(NMR)	M_w(GPC)	M_n(GPC)	M_n(NMR)
G-1	0.69	0.89	0.67	−7.90	−7.32	−8.04	0.994	0.993	0.983
G-2	0.72	0.76	0.65	−7.74	−7.69	−8.04	0.983	0.986	0.979
average	0.70 ± 0.02	0.83 ± 0.07	0.66 ± 0.01	−7.82 ± 0.08	−7.51 ± 0.19	−8.04 ± 0.00			
kraft (Fr1−Fr9)[b]	0.59	[c]	[d]	−8.21	[c]	[d]	0.969	[c]	[d]

[a]The average scaling factors are given with the associated standard deviation. The parameters were measured on 86 mg mL^{-1} solutions of the fractions. The probe temperature was maintained at 295 K. Average diffusion coefficients were used in the diffusion dimension of the chart. For polymer **Ac-1(V)**, these were obtained by selecting 21 peaks for each fraction spectra and taking the average of the calculated diffusion coefficients of these peaks. For kraft lignin, these were obtained by selecting only eight peaks for each fraction spectra because of the broadness of the signals. [b]Scaling factors of combined kraft lignin fractions that adhere to the average trend shown for the G-1 and G-2 fractionations. [c]Unsatisfactory linear correlation was obtained. [d]End groups of kraft lignin were not resolved in ^{1}H NMR. Data were not obtained.

DOI: 10.1021/acsomega.7b01287
ACS Omega 2017, 2, 8466−8474

observed regions was estimated to be at fraction F8. The fraction yield profiles of KL-1 and KL-2 were similar (Figure 4), showing the good reproducibility of the process.

Analysis of the Fractions Derived from the Commercially Available Kraft Lignin. GPC analysis of the 14 fractions showed that M_w steadily increased across the fractions from 900 (5% KL-1) to 10 300 (70% KL-2) g mol^{-1} (Table S12). No significant differences in the M_w values were found for the corresponding fractions between KL-1 and KL-2 fractionations (Table S12). However, considerable discrepancies were found for the M_n values. For fractions F1−F8, M_n and M_w values showed a trend analogous to that obtained for **Ac-1(V)**, with the $Đ_M$ values ranging from 1.5 to 2 (Table S12). As the M_n values became more variable after fraction F8, the calculated $Đ_M$ values become considerably larger (Table S12). Moreover, a significant difference in the M_n values obtained was observed for the two fractionations (KL-1 and KL-2, Table S11). The threshold observed for the discrepancies of the M_n values seems to correlate quite closely with the one between the two regions proposed in the fraction yield profile (Figure 4). It was not possible to determine the M_n values by quantitative ^{1}H NMR end-group analysis as signals for the end groups were not apparent in the 1D ^{1}H NMR spectra.

As the M_w values were relatively consistent across all fractions, data from both fractionations were combined and fitted to the Mark−Houwink eq 1 against the average values of the diffusion coefficient obtained for each fraction by DOSY NMR (Figure 5). For fractions F1−F10, a linear correlation

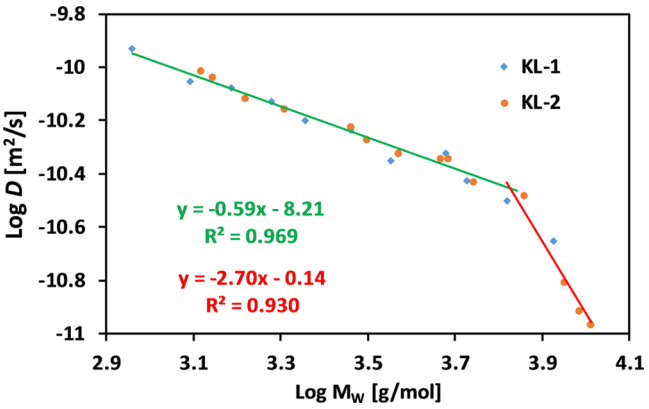

Figure 5. Scaling of diffusion coefficients with the MW kraft fractions (blue: KL-1 and red: KL-2). The green trend line corresponds to the combination of fractions F1−F10 from both KL-1 and KL-2 fractionations. The red trend line corresponds to the combination of fractions F11−F14 from both fractionations. Linear equations and R^2 values are color-coded for the trend line they correspond to.

was obtained with R^2 = 0.969. The scaling factor (α = 0.59) is slightly lower than the empirical scaling derived for the model polymer **Ac-1(V)** (α = 0.66 ± 0.01). These findings imply that lighter fractions of kraft lignin could be composed of chains similar to polymer **Ac-1(V)** rather than heavily branched macromolecules.[23] Surprisingly, some recent results of the analysis of kraft lignin fractions suggest the opposite.[10,22] This could be possibly explained by the difference in fractionation methods or a different source of kraft lignin with a different degree of condensation and branching.

After fraction F11, there was a dramatic divergence from the F1−F10 linear polymer region and a sudden increase in the scaling of the diffusion coefficient with MW was observed. The trend is opposite to the one that would be expected in the case of extensive branching (condensation) of lignin macromolecules. The unphysically large scaling exponent in this region is likely artifactual. However, there might be possible explanations for this phenomenon that still provide information about the polymer. We suppose that the M_w values that were determined by GPC might be underestimated. It is known that branched lignin macromolecules have smaller hydrodynamic radii than the random-coil polystyrene GPC standards of the same MW and therefore elute with longer retention times.[39] Consequently, any efforts to make cross comparisons of volume−MW relationships between lignin and other polymers might be subject to substantial errors. Unfortunately, without a reliable alternative means of determining the MW of lignin fractions at our disposal, we are not able to confirm this hypothesis. Another source of error could stem from limitations in the DOSY NMR method. The analysis has been carried out using standard equipment that can deliver gradient pulses of limited strength. The inability to apply strong enough gradient pulses was compensated for by using very long diffusion delays. This could possibly result in the overestimation of the D values for heavier fractions of lignin. Repeating the experiments using a specialized diffusion NMR equipment could possibly clarify this issue.

To support our hypothesis that kraft lignin is composed of two components with different physical properties, the fractions were analyzed further by another magnetic resonance method. One-dimensional ^{1}H NMR spectra did not show any considerable differences across the fractions apart from the expected broadening of resonances for heavier fractions (Figure S8). Likewise, qualitative comparison of HSQC spectra did not reveal any insights into the proposed two types of kraft lignin. However, collation of absolute integrals showed a steady decline of cross-peak intensities toward heavier fractions which can be related to the dependence of T_1 and T_2 relaxation times on mobility and size of the molecules (Figure 6). Another interesting phenomenon becomes apparent when intensities of the cross-peaks (b) and (c) are compared. These cross-peaks represent a diastereotopic pair of protons hence should show

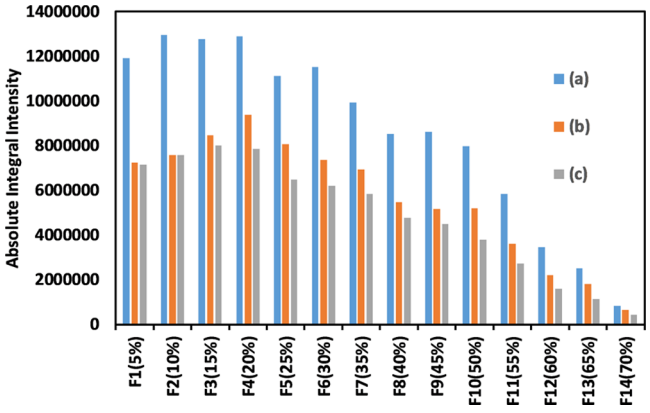

Figure 6. Absolute integral intensities of selected cross-peaks in the HSQC spectra of kraft lignin fractions (KL-2). (a) α proton β-O-4 linkage δ_C/δ_H—73.2−75.6/6.01−5.864, (b) γ-1 proton $\beta-\beta$ linkage δ_C/δ_H—71.7/4.2, and (c) γ-2 proton $\beta-\beta$ linkage δ_C/δ_H—71.7/3.9. The decline toward heavier fractions clearly demonstrates the effect of MW on the intensities of HSQC cross-peaks caused by the dependence of T_1 and T_2 relaxation times on mobility and size of the molecules.

DOI: 10.1021/acsomega.7b01287
ACS Omega 2017, 2, 8466−8474

equal intensity (for assignment, see Figure S9). This holds true only for the two lightest fractions. The differences observed in heavier fractions are likely created by the effect of restricted local mobility on relaxation times. These findings imply that HSQC spectra of unfractionated lignin with a high $Đ_M$ value are dominated by the resonances of lighter fractions and might not represent the true overall structure of lignin. The effect of T_1 relaxation time can certainly be diminished by the use of relaxation agents and/or an increased interscan delay. However, using a relaxation delay of 15 s, that would assure, according to our measurements, full longitudinal relaxation of all ^{1}H resonances in unfractionated polydisperse samples of lignin, makes the HSQC experiment very long and unpractical (see Figure S10). Furthermore, the effect of the T_2 relaxation time on the INEPT transfer in the HSQC methods cannot be corrected.[12] From this perspective, any attempts to use HSQC spectra in a quantitative manner for lignin characterization are questionable and the need to combine fractionation methods with other means of characterization for the analysis of such complex materials as kraft lignin becomes even more apparent.

Seeking further evidence for the differences between the fractions of kraft lignin lead us to use continuous-wave EPR spectroscopy. It is known that lignin isolated from biomass contains significant amounts of stable organic radicals, and therefore EPR spectroscopy has become an increasingly popular method for the characterization of this material.[40,41] The results from the measurement of radical concentrations in samples of crude, acetylated, and fractionated kraft lignin are summarized in Figure 7. Comparison of the values obtained for

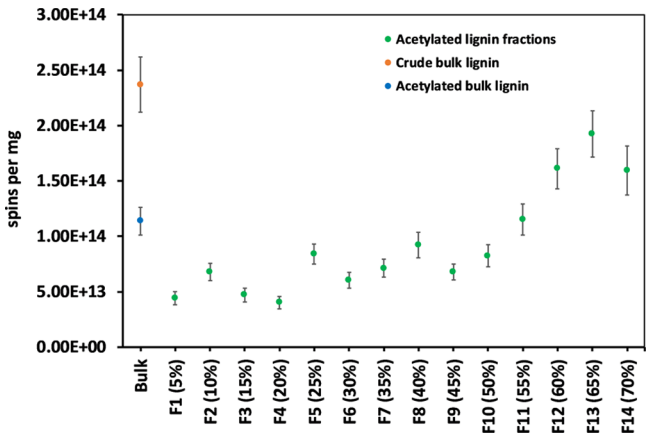

Figure 7. Radical concentrations in spins per mg of sample mass for crude, acetylated bulk kraft lignin and appropriate fractions. Uncertainties in the number of spins per milligram of sample were estimated from the respective weighing and volumetric errors and the corrected standard deviations of triplicate measurements propagated to spins per weight.

crude and acetylated bulk samples implies that acetylation of kraft lignin decreased the concentration of free radicals by a factor of about 2. It is generally assumed that the sources of unpaired electrons in lignin are semiquinone radicals stabilized in the polyphenolic lignin matrix. Upon acetylation, the number of phenolic hydroxyl groups should be considerably reduced which is in accordance with diminishing radical concentration per milligram. However, the remaining radical content likely implies that the acetylation of the bulk lignin sample was not fully accomplished. For only lighter acetylated lignin fractions (F1–F10), the radical concentration is rather low (below 1×10^{14}) and only a subtle increase with MW is apparent. On the contrary, the heavy fractions (F11–F14) show radical concentrations above the one that was found for the bulk acetylated lignin. We assume that one possible explanation could be that the lower reactivity of phenolic groups in the heavier fractions results in a lower degree of acetylation. However, we are currently unable to make an unambiguous conclusion about this phenomenon as radical concentrations in unacetylated kraft lignin fractions are unknown. Nevertheless, the threshold between heavy and light fractions roughly correlates with that suggested previously based on the fractionation yield profile (Figure 4) and DOSY NMR analysis (Figure 5). Hence, we assume that the results of EPR analysis support the hypothesis that two very different components of kraft lignin exist.

EXPERIMENTAL SECTION

All NMR analyses of polymer and lignin samples were carried out using a Bruker 700 MHz spectrometer equipped with a nitrogen-cooled TCI CryoProbe (Prodigy). The samples were prepared by dissolving 60 mg of material in 0.7 mL of DMSO-d_6. The samples were then sonicated for 30 min at 35 °C and then filtered through a 0.45 μm poly(tetrafluoroethylene) syringe filter. Quantitative ^{1}H NMR spectra were acquired with the standard pulse sequence from the Bruker library (*zg*) and used a 30 s interscan (D_1) delay. HSQC spectra were acquired using the *hsqcetgpsp.2* pulse sequence with a spectral width of 86 ppm and 126 points in the indirect dimension (D_1 = 1 s, ns = 12) and a total experimental time of 30 min.

DOSY experiments were acquired using the *ledbpgp2s* pulse sequence. Gradient amplitude (6.56 G mm^{-1}) was calibrated using the residual signal of HDO in D_2O sample. The diffusion delay (Δ) and gradient pulse length (δ) were optimized for each sample to achieve ca. 5–10% residual signal at 98% gradient strength (compared to 10% gradient strength) using the 1D DOSY experiment with the *ledbpgp2s1d* pulse sequence. Each *pseudo*-2D experiment consisted of a series of 32 spectra acquired with 65 536 data points. The gradient pulses were incremented from 10 to 98% with a linear ramp. All samples were allowed to thermally equilibrate prior to optimizing the DOSY parameters (Δ and δ), and the temperature was set and maintained at 295 K during the experiments. Data sets were processed by Fourier transformation in F_2, using a line broadening of 10 Hz, followed by a baseline correction. The DOSY analysis was then performed in Bruker Dynamics Center 2.3. Manual peak picking was performed for each data set, and the peak intensities were used to measure the signal decay. Error estimation of the fit was performed at 95% confidence level. Further particulars of the DOSY NMR method can be found in Figure S6.

Experimental details for the synthesis of the model polymer and other analytical methods employed in this study are given in the Supporting Information.

CONCLUSIONS

In this study, we have described an optimized scalable synthesis of **1**. The resulting polymer was acetylated to increase its solubility and then completely fractionated using the volatile organic solvents acetone and diethyl ether, with no insoluble fraction being produced. This was achieved by using incremental increases in the percentage of acetone up to 45%, leading to a series of fractions that were then analyzed by

DOI: 10.1021/acsomega.7b01287
ACS Omega 2017, 2, 8466–8474

GPC, ^{1}H end-group analysis, and DOSY NMR. Good linear log−log correlations of the average diffusion coefficient and average MWs M_w and M_n were obtained. The average molecular scaling exponent $\alpha = 0.66 \pm 0.01$ corresponds to a flexible linear polymer in a good solvent and could be possibly used as an empirical Mark−Houwink parameter for a quick DOSY NMR assessment of the MW of light fractions of unbranched lignin. Although GPC is well established in polymer chemistry, some findings in this paper suggest that it might not work that well for lignin samples that are composed of smaller, oligomer-like (ca. up to 10 kDa), molecules and/or have rather heterogeneous character. Therefore, we believe that the DOSY NMR method could possibly deliver faster and more accurate results.

This concept was explored further through the use of a commercial sample of kraft lignin which was fractionated using the same protocol. In this case, higher concentrations of acetone had to be used to fractionate the whole bulk material and a greater number of fractions were obtained. A clear threshold was observed in the fraction yield analysis, showing that the majority of kraft lignin (about 70%) was dissolved using concentrations of acetone higher than 45%. For the lighter fractions of kraft lignin, scaling of diffusion coefficients with MW ($\alpha = 0.59$) is very similar to that observed for **Ac-1(V)** which leads to the conclusion that these fractions are primarily made of linear flexible macromolecules. The sudden change in α, observed for the heavy fractions (F11−F14), implies that the bulk material of the acetylated kraft lignin might be composed of a second component with significantly different physical properties. This hypothesis is supported by the results of continuous-wave EPR spectroscopy that show a significant increase in the radical concentration for the heavy fractions. Although we are unable to make unambiguous conclusions about the precise structural differences at this time, we assume that lighter fractions of lignin are made of smaller molecules with simpler linear structures that could be more suitable materials for exploring lignin depolymerization reactions than the crude unfractionated lignin.

■ ASSOCIATED CONTENT

Supporting Information

The Supporting Information is available free of charge on the ACS Publications website at DOI: 10.1021/acsomega.7b01287.

Experimental procedures, additional experiments, and novel compound data (PDF)

■ AUTHOR INFORMATION

Corresponding Authors

*E-mail: njw3@st-andrews.ac.uk (N.J.W.).
*E-mail: tl12@st-andrews.ac.uk (T.L.).

ORCID

Bela E. Bode: 0000-0002-3384-271X
Nicholas J. Westwood: 0000-0003-0630-0138
Tomas Lebl: 0000-0002-0269-3221

Author Contributions

The manuscript was written through the contributions of all authors. All authors have given approval to the final version of the manuscript.

Notes

The authors declare no competing financial interest.

■ ACKNOWLEDGMENTS

This work was supported by EPSRC Ph.D. studentships (EP/1518175 (DMB)), the Industrial Biotechnology Innovation Centre (Ph.D. studentship to DMB), and an EPSRC Doctoral Prize Fellowship (CSL). We also acknowledge the EPSRC UK Mass Spectrometry Facility at Swansea University for mass spectrometry analysis. We would like to thank Drs. Alison Woodward, Sankar Meenakshisundaram, Mario De Bruyn, Krisztina Kovacs-Schreiner, Gary Sheldrake, and Professor Gillian Stephens for inspiring us to focus on the synthesis of all-G β-O-4 polymer **1** and LBNet for a Proof-of-Concept grant that helped us all to collaborate. We would also like to thank Adam Sinclair for his input.

■ ABBREVIATIONS

DP, degree of polymerization; DHPs, dehydrogenase polymers; DOSY, diffusion-ordered spectroscopy; GPC, gel permeation chromatography; HSQC, heteronuclear single-quantum coherence; MALDI-TOF-MS, matrix-assisted laser desorption ionization time-of-flight mass spectrometry; M_n, number average molecular weight; M_w, weight average molecular weight; NMR, nuclear magnetic resonance; PFG, pulsed field gradient; PS, polystyrene; TLC, thin-layer chromatography; UV, ultraviolet; wt %, weight percent.

■ REFERENCES

(1) Rinaldi, R.; Jastrzebski, R.; Clough, M. T.; Ralph, J.; Kennema, M.; Bruijnincx, P. C. A.; Weckhuysen, B. M. Paving the Way for Lignin Valorisation: Recent Advances in Bioengineering, Biorefining and Catalysis. *Angew. Chem., Int. Ed.* **2016**, *55*, 8164−8215.

(2) Deuss, P. J.; Lahive, C. W.; Lancefield, C. S.; Westwood, N. J.; Kamer, P. C. J.; Barta, K.; de Vries, J. G. Metal Triflates for the Production of Aromatics from Lignin. *ChemSusChem* **2016**, *9*, 2974−2981.

(3) Rahimi, A.; Ulbrich, A.; Coon, J. J.; Stahl, S. S. Formic-acid-induced depolymerization of oxidized lignin to aromatics. *Nature* **2014**, *515*, 249−252.

(4) Zhao, S.; Abu-Omar, M. M. Synthesis of Renewable Thermoset Polymers through Successive Lignin Modification Using Lignin-Derived Phenols. *ACS Sustainable Chem. Eng.* **2017**, *5*, 5059−5066.

(5) Yang, Y.; Deng, Y.; Tong, Z.; Wang, C. Renewable lignin-based xerogels with self-cleaning properties and superhydrophobicity. *ACS Sustainable Chem. Eng.* **2014**, *2*, 1729−1733.

(6) Atifi, S.; Miao, C.; Hamad, W. Y. Surface modification of lignin for applications in polypropylene blends. *J. Appl. Polym. Sci.* **2017**, *134*, 45103.

(7) Shuai, L.; Amiri, M. T.; Questell-Santiago, Y. M.; Héroguel, F.; Li, Y.; Kim, H.; Meilan, R.; Chapple, C.; Ralph, J.; Luterbacher, J. S. Formaldehyde stabilization facilitates lignin monomer production during biomass depolymerization. *Science* **2016**, *354*, 329−333.

(8) Lancefield, C. S.; Ojo, O. S.; Tran, F.; Westwood, N. J. Isolation of functionalized phenolic monomers through selective oxidation and C−O bond cleavage of the β-O-4 linkages in lignin. *Angew. Chem., Int. Ed. Engl.* **2015**, *54*, 258−262.

(9) Deuss, P. J.; Lancefield, C. S.; Narani, A.; de Vries, J. G.; Westwood, N. J.; Barta, K. Phenolic acetals from lignins of varying compositions via iron(iii) triflate catalysed depolymerisation. *Green Chem.* **2017**, *19*, 2774.

(10) Crestini, C.; Lange, H.; Sette, M.; Argyropoulos, D. S. On the structure of softwood kraft lignin. *Green Chem.* **2017**, *19*, 4104−4121.

(11) Sette, M.; Wechselberger, R.; Crestini, C. Elucidation of Lignin Structure by Quantitative 2D NMR. *Chem.—Eur. J.* **2011**, *17*, 9529−9535.

(12) Zhang, L.; Gellerstedt, G. Quantitative 2D HSQC NMR determination of polymer structures by selecting suitable internal standard references. *Magn. Reson. Chem.* **2007**, *45*, 37−45.

DOI: 10.1021/acsomega.7b01287
ACS Omega 2017, 2, 8466−8474

(13) Duval, A.; Vilaplana, F.; Crestini, C.; Lawoko, M. Solvent screening for the fractionation of industrial Kraft lignin. *Holzforschung* **2016**, *70*, 1−94.
(14) Toledano, A.; Serrano, L.; Garcia, A.; Mondragon, I.; Labidi, J. Comparative study of lignin fractionation by ultrafiltration and selective precipitation. *Chem. Eng. J.* **2010**, *157*, 93−99.
(15) Boeriu, C. G.; Fiţigău, F. I.; Gosselink, R. J. A.; Frissen, A. E.; Stoutjesdijk, J.; Peter, F. Fractionation of five technical lignins by selective extraction in green solvents and characterisation of isolated fractions. *Ind. Crops Prod.* **2014**, *62*, 481−490.
(16) Lange, H.; Schiffels, P.; Sette, M.; Sevastyanova, O.; Crestini, C. Fractional Precipitation of Wheat Straw Organosolv Lignin: Macroscopic Properties and Structural Insights. *ACS Sustainable Chem. Eng.* **2016**, *4*, 5136−5151.
(17) Sadeghifar, H.; Argyropoulos, D. S. Macroscopic Behavior of Kraft Lignin Fractions: Melt Stability Considerations for Lignin−Polyethylene Blends. *ACS Sustainable Chem. Eng.* **2016**, *4*, 5160−5166.
(18) Sadeghifar, H.; Argyropoulos, D. S. Correlations of the Antioxidant Properties of Softwood Kraft Lignin Fractions with the Thermal Stability of Its Blends with Polyethylene. *ACS Sustainable Chem. Eng.* **2015**, *3*, 349−356.
(19) Lan, W.; Rencoret, J.; Lu, F.; Karlen, S. D.; Smith, B. G.; Harris, P. J.; del Río, J. C.; Ralph, J. Tricin-Lignins: Occurrence and Quantitation of Tricin in Relation to Phylogeny. *Plant J.* **2016**, *88*, 1046−1057.
(20) Lange, H.; Rulli, F.; Crestini, C. Gel Permeation Chromatography in Determining Molecular Weights of Lignins: Critical Aspects Revisited for Improved Utility in the Development of Novel Materials. *ACS Sustainable Chem. Eng.* **2016**, *4*, 5167−5180.
(21) Li, W.; Chung, H.; Daeffler, C.; Johnson, J. A.; Grubbs, R. H. Application of ^{1}H DOSY for Facile Measurement of Polymer Molecular Weights. *Macromolecules* **2012**, *45*, 9595−9603.
(22) Rönnols, J.; Jacobs, A.; Aldaeus, F. Consecutive determination of softwood kraft lignin structure and molar mass from NMR measurements. *Holzforschung* **2017**, *71*, 543−680.
(23) Garver, T. M.; Callaghan, P. T. Hydrodynamics of kraft lignins. *Macromolecules* **1991**, *24*, 420−430.
(24) Norgren, M.; Lindström, B. Physico-chemical characterization of a fractionated kraft lignin. *Holzforschung* **2000**, *54*, 449−562.
(25) Ito, T.; Hayase, R.; Kawai, S.; Ohashi, H.; Higuchi, T. Coniferyl aldehyde dimers in dehydrogenative polymerization: model of abnormal lignin formation in cinnamyl alcohol dehydrogenase-deficient plants. *J. Wood Sci.* **2002**, *48*, 216−221.
(26) Kishimoto, T.; Uraki, Y.; Ubukata, M. Synthesis of *β*-O-4-type artificial lignin polymers and their analysis by NMR spectroscopy. *Org. Biomol. Chem.* **2008**, *6*, 2982.
(27) Kishimoto, T.; Uraki, Y.; Ubukata, M. Synthesis of Bromoacetophenone Derivatives as Starting Monomers for *β*-O-4 Type Artificial Lignin Polymers. *J. Wood Chem. Technol.* **2008**, *28*, 97−105.
(28) Lancefield, C. S.; Westwood, N. J. The synthesis and analysis of advanced lignin model polymers. *Green Chem.* **2015**, *17*, 4980−4990.
(29) Tolbert, A.; Akinosho, H.; Khunsupat, R.; Naskar, A. K.; Ragauskas, A. J. Characterization and analysis of the molecular weight of lignin for biorefining studies. *Biofuels, Bioprod. Biorefin.* **2014**, *8*, 836−856.
(30) Cui, C.; Sun, R.; Argyropoulos, D. S. Fractional Precipitation of Softwood Kraft Lignin: Isolation of Narrow Fractions Common to a Variety of Lignins. *ACS Sustainable Chem. Eng.* **2014**, *2*, 959−968.
(31) Sette, M.; Lange, H.; Crestini, C. Quantitative HSQC Analyses of Lignin: a Practical Comparison. *Comput. Struct. Biotechnol. J.* **2013**, *6*, No. e201303016.
(32) Burdick, J. A.; Lovestead, T. M.; Anseth, K. S. Kinetic chain lengths in highly cross-linked networks formed by the photoinitiated polymerization of divinyl monomers: A gel permeation chromatography investigation. *Biomacromolecules* **2003**, *4*, 149−156.
(33) Izunobi, J. U.; Higginbotham, C. L. Polymer Molecular Weight Analysis by ^{1}H NMR Spectroscopy. *J. Chem. Educ.* **2011**, *88*, 1098−1104.
(34) Flory, P. J. *Principles of Polymer Chemistry*; Cornell University Press, 1953; pp 595−657.
(35) Doi, M.; Edwards, S. F. *The Theory of Polymer Dynamics*; Oxford University Press, 1990; pp 91−139.
(36) Rosenboom, J.-G.; De Roo, J.; Storti, G.; Morbidelli, M. Diffusion (DOSY) ^{1}H NMR as an Alternative Method for Molecular Weight Determination of Poly(ethylene furanoate) (PEF) Polyesters. *Macromol. Chem. Phys.* **2016**, *218*, 1600436.
(37) Guo, X.; Laryea, E.; Wilhelm, M.; Luy, B.; Nirschl, H.; Guthausen, G. Diffusion in Polymer Solutions: Molecular Weight Distribution by PFG-NMR and Relation to SEC. *Macromol. Chem. Phys.* **2017**, *218*, 1600440.
(38) Chamignon, C.; Duret, D.; Charreyre, M.-T.; Favier, A. ^{1}H DOSY NMR Determination of the Molecular Weight and the Solution Properties of Poly(N-acryloylmorpholine) in Various Solvents. *Macromol. Chem. Phys.* **2016**, *217*, 2286−2293.
(39) Himmel, M. E.; Oh, K. K.; Quigley, D. R.; Grohmann, K. Alkaline size-exclusion chromatography of lignins and coal extracts using cross-linked dextran gels. *J. Chromatogr. A* **1989**, *467*, 309−314.
(40) Patil, S. V.; Argyropoulos, D. S. Stable Organic Radicals in Lignin: A Review. *ChemSusChem* **2017**, *10*, 3284−3303.
(41) Bährle, C.; Nick, T. U.; Bennati, M.; Jeschke, G.; Vogel, F. High-Field Electron Paramagnetic Resonance and Density Functional Theory Study of Stable Organic Radicals in Lignin: Influence of the Extraction Process, Botanical Origin, and Protonation Reactions on the Radical g Tensor. *J. Phys. Chem. A* **2015**, *119*, 6475−6482.

DOI: 10.1021/acsomega.7b01287
ACS Omega 2017, 2, 8466−8474